Low-profile inductive metasurface for surface wave excitation in L-band: design, manufacture and electromagnetic infrared measurements

André Barka[1], Daniel Prost[1]
[1]ONERA/DEMR, Université de Toulouse, France. ONERA is the French Aerospace Lab and DEMR its ElectroMagnetism and Radar Department.
Corresponding author: André Barka (e-mail: andre.barka@onera.fr)

ABSTRACT This paper describes a low profile inductive surface for High Frequency Surface Wave Radars (HFSWR). The long-term operating frequency band considered is High Frequency (HF). In this paper we will only discuss L-band in order to simplify the manufacturing phase and the proof of concept. A compact thin 2D Super Inductive Surface (SIS) based on printed metal rings excited by an L-band monopole (1.1 GHz) is proposed to significantly increase (10 dB at the extremity of the SIS and 7 dB at one wavelength further) an electric field in TM polarization (electric field normal at the air/sea interface) required to excite a surface wave. The proposed SIS thickness 10.26 mm ($\frac{\lambda}{30}$), is approximatly three times thinner than a recent 3D SIS developed both in L-band and HF-band ($\frac{\lambda}{10}$) which makes it possible to consider surface wave launchers of much lower height in the HF-band in the future. A 2D L-band prototype with a bandwidth of 130 MHz was manufactured and ElectroMagnetic Infrared measuRements (EMIR) confirmed simulated SIS performances.

INDEX TERMS High Frequency Surface Wave Radars (HFSWR), sea surface wave, High Frequency (HF), L band, Inductive surface

I. INTRODUCTION

HIGH Frequency Surface Wave Radars (HFSWR) are of great interest as a solution for the surveillance of the Exclusive Economic Zone, a portion of the sea that can be extended by states up to 200 nautical miles from the seashore [1]. Operating in the high frequency (HF) band, namely from 3 MHz to 30 MHz, their coverage is not limited by the radio horizon. It is communly known that the HFSWR's range can exceed 300 km with antennas placed at ground level, while the range of an X-band maritime radar is around 40 km, with the antenna placed a few tens of meters away from above. It should be noted that, although operating systems exist with good performances, HFSWRs have one major problem: only a minor part of the energy radiated by the transmitting antennas is conveyed at the sea surface. Less than 50 percent of the power available in the source is radiated as a surface wave. In [2] the excitation of a surface wave from short vertical antennas is analytically given and in [3], [4], [9], [10] , the parameters required by a surface to propagate mainly a sole Transverse Magnetic (TM) surface wave by minimizing the volume "sky" waves have been determined. This specific surface called a Super Inductive Surface (SIS):

- increases the energy carried by the surface wave,
- induces a propagation focused at the interface
- causes no sky wave excitation.

An initial 3D concept composed of perfectly conductive vertical plates arranged on a ground plane was proposed funded a French patent [11] and a first model proof of concept was produced in L-band. A 10 dB field amplification produced by the inductive SIS surface was verified experimentally. However, this device, which is very effective for exciting surface wave, has a significant thickness of 0.1074 λ. In this letter we propose a simple, more compact 2D low-profile inductive unit-cell (Fig. 1) which is about three times thinner (0.037 λ) while maintaining a 10 dB field amplification. The electric equivalent model at normal incidence is provided and discussed showing the inductive behavior of the metasurface. The design and manufacture of the L-band inductive surface is fully described in Section II, while Section III contains the experimental validation results obtained by Electromagnetic Infrared Measurements (EMIR).

II. METASURFACE DESIGN AND MANUFACTURE

The proposed 2D super inductive surface is shown schematically in Fig. 2, and Table 1 lists its dimensions according to wavelength. The very small dimensions in terms of wavelength of the proposed device confer the properties of a metasurface. The metasurface consists of a regular grid made

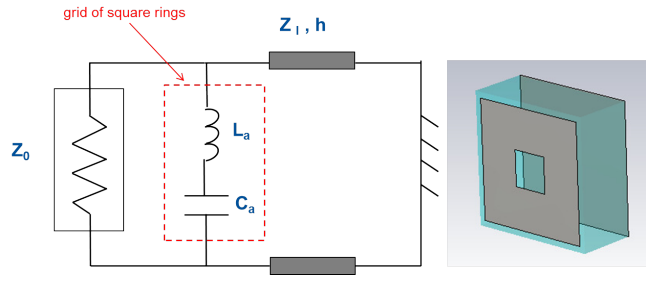

FIGURE 1. SIS unit-cell

up of N_x = 12 and N_y = 5 metal rings. Lattice periodicity is p = 0.128 λ. The metasurface's metal cells are printed on a Rogers TMM6 substrate of thickness h = 0.037 λ (ϵ_r = 6, tg δ = 0.0023). The in-plane thickness of the rings is e = 0.04 λ, and the gap between two rings is g = 0.012 λ. The total length of the SIS launcher is equal to Lx = 1.535 λ and its width is equal to Ly = 0.64 λ.

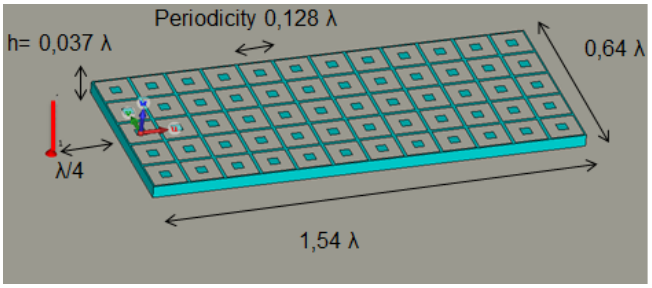

FIGURE 2. Dimensions of the L-band SIS mockup

TABLE 1. Main SIS parameters

SIS mockup parameters	
(N_x,N_y)	(12, 5)
Periodicity (p)	0.128 λ
ring thickness (e)	0.04 λ
ring gap (g)	0.012 λ
Rogers TMM6 thickness (h)	0.037 λ
Rogers TMM6 permittivity (ϵ_r)	6
Rogers TMM6 losses(tg δ)	0.0023
SIS surface	1.54 λ x 0.64 λ

In order to determine and design the strongly inductive property of the metasurface, we proposed an equivalent circuit defined for incident waves perpendicular to the metasurface (Fig. 1). In the proposed structure, the array of square metallic rings functions as capacitors (C_a) and inductances (L_a) in series. The impedance of the grid is then given:

$$Z_a = j\omega L_a + \frac{1}{j\omega C_a} \tag{1}$$

We used simplified models of the capacitors and inductances given by [8]:

$$C_a = \frac{\mu_0}{\pi}(p-g)\ln(csc(\frac{\pi e}{p})) \tag{2}$$

and

$$L_a = \frac{2\epsilon_e\epsilon_0}{2\pi}(p-g)\ln(csc(\frac{\pi g}{2p})) \tag{3}$$

where $\epsilon_e = \frac{1+\epsilon_r}{2}$. A dielectric substrate of length h, backed by a ground plane is connected in parallel with the metal grid. It is represented by a transmission line with the characteristic impedance of:

$$Z_s = jZ_0\sqrt{\frac{\mu_r}{\epsilon_r}}\tan(k_0\sqrt{\epsilon_r\mu_r}h). \tag{4}$$

Fig. 3 represents the evolution of the equivalent impedance

$$Z_e = \frac{Z_a Z_s}{Za + Z_s} \tag{5}$$

according to thickness h of the substrate. It is observed that Z_e is a purely imaginary complex, positive before resonance (between 11 mm and 12 mm), which confers a Super Inductive Surface (SIS) property to the metamaterial. Following resonance, the imaginary part of the equivalent impedance becomes negative, and the metasurface then has a capacitive behavior.

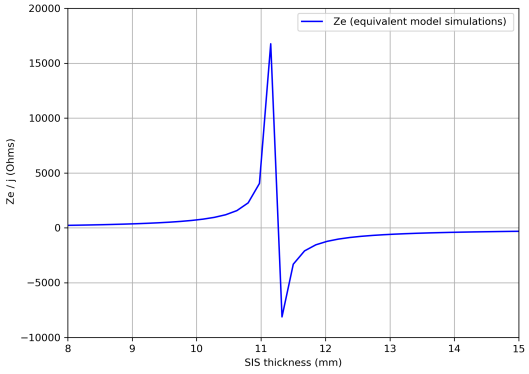

FIGURE 3. Imaginary part of the SIS equivalent impedance

In our application, the SIS is excited by a quarter-wavelength monopole antenna making it possible to radiate an electric field in vertical polarization (TM polarization) and thus exciting, together with the SIS, a surface wave above the sea. A quarter-wavelength monopole tuned to 1.1 GHz, is placed on a ground plane, 0.25 λ from the metasurface. We carried out SIS optimization phases (using CST Microwave Studio electromagnetic full-wave calculation software [5]) in the L-band at the transmission frequency of 1.1 GHz. Absorbing boundary conditions of CST (open add space) are implemented on the exterior boundary of the computational domain. Our simulations systematically recorded the electric field's vertical component. This is, in fact, the main component of the field radiated by the excitation antenna used. The effect of the planar SIS is evaluated from its electric field gain. This gain is calculated by the amplitude ratio of the vertical component of the electric field E_{SIS} in the presence of the SIS divided by the amplitude E_i of the vertical

component of the electric field radiated by the monopole alone (gain = 20 log ($\frac{E_{SIS}}{E_i}$)). Fig. 4 shows that the operating bandwidth of the manufactured SIS is approximately 130 MHz. Both simulations and Vector Network Analyzer (VNA) measurements show that the SIS creates ripples on the reflection coefficient curves, due to the reflection phenomena at the extremity of the metasurface. A slight shift of about 50 MHz in the operating frequency is observed. We attribute this to a slight difference in monopole height, and not to the SIS. A gain simulation of the monopole antenna with the SIS clearly shows, in Fig. 5, that the beam is oriented along the horizontal axis x with a maximum level of 10.3 dBi for an azimuth angle of θ =90°. By the way of comparison, the gain of the same monopole antenna installed on a ground plane of same dimension is 5.2 dBi (Fig. 5). We also observed in Fig. 5, that the SIS is responsible for higher cross-polarization levels (up to 20 dB) but they remain limited to -20 dB.

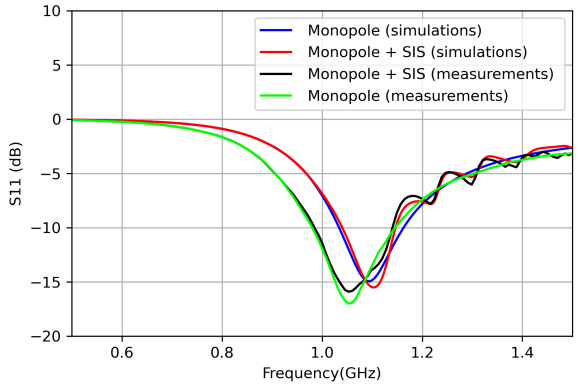

FIGURE 4. Reflection coefficient of the SIS mockup comprising two Rogers TMM6 layers (measurements and simulations)

Based on an initial CST parametric study in the horizontal and vertical planes (Fig. 6 and Fig. 7), we observed that the optimum substrate thickness giving the maximum gain was about 11 mm, very close to the optimal thickness predicted by the equivalent circuit in Fig. 3. Indeed, the simulations show, both in Fig. 6 and Fig. 7, that the gains are very low for a substrate thickness of 5 mm (blue) and increase significantly up to a 11 mm thickness (pink) for which the metasurface remains inductive. Following resonance, the surface becomes capacitive (the imaginary part of Z_e is negative) resulting in a strong decrease of the gain. The proposed SIS design, based on a grid of square rings, then reproduces a high inductive surface fairly well. A second parametric study showed that it is very important to control the losses in the substrate separating the SIS from the ground plane. We then carried out simulations for which the conductivity of the substrate varied between $\sigma = 10^{-5}$ S/m and $\sigma = 10^{-3}$ S/m. Indeed, a too high level of losses in the substrate ($\sigma = 10^{-3}$ S/m) canceled out the effect of the ground plane and considerably reduced the SIS amplification levels.

In order to get as close as possible to the theoretical

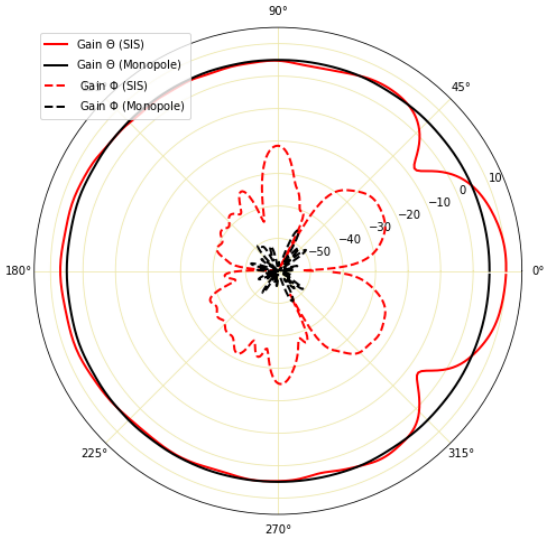

FIGURE 5. Co and cross polarization simulated Gain pattern at 1.1 GHz; Monopole+SIS (red curve), Monopole (black curve)

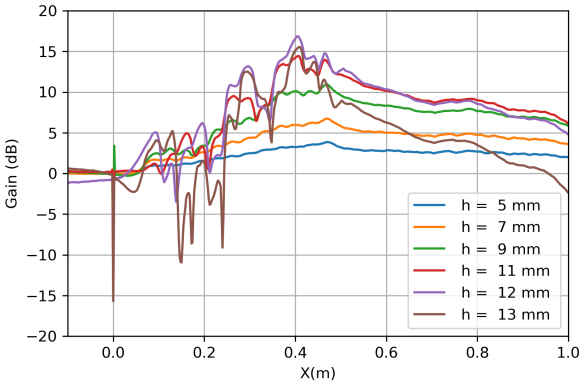

FIGURE 6. Simulated horizontal gain versus substrate thickness along a line lying in the horizontal plane (near field raised 3 cm above the ground plane)

thickness of 11 mm predicted by simulation, the SIS mockup operating in the L-band (Fig. 10) was manufactured by CIRETEC [6] with two 5.08 mm thick layers of Rogers TMM6 [7] (ϵ =6 and tg δ=0.0023) glued with a 0.1 mm thick pre-preg RO4406G2 (ϵ = 6.15 and tg δ = 0.004). The metal rings and the group plane are made of 18-micron thick copper. The total thickness of the manufactured SIS is 10.26 mm ($\frac{\lambda}{27}$ at 1.1 GHz).

III. ELECTROMAGNETIC INFRARED MEASUREMENTS

EMIR measurement facility was used to verify the confinement of the electric field at the air-to-ground interface. The EMIR method was introduced in the 90s at the French Aerospace Lab ONERA [12], [13], and is widely used to characterize High Impedance Surfaces (HIS) [14], [15]. This

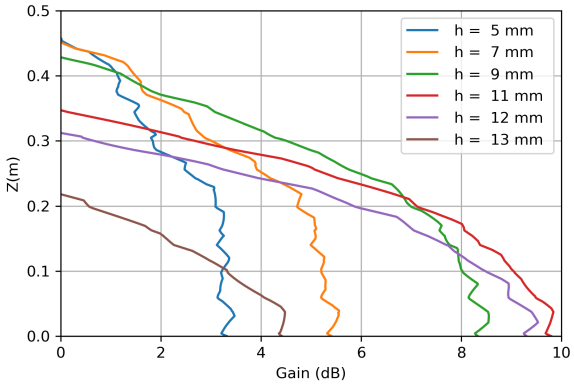

FIGURE 7. Simulated vertical gain versus substrate thickness along a line lying in the vertical plane at X = 59 cm from the monopole

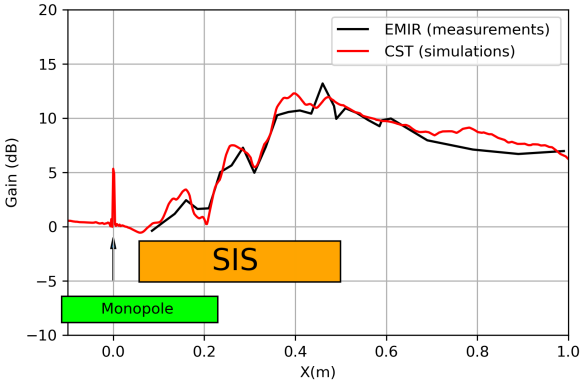

FIGURE 8. Simulated and measured gain at 1.1 GHz along a line lying in the horizontal plane (near field raised 3 cm above the ground plane)

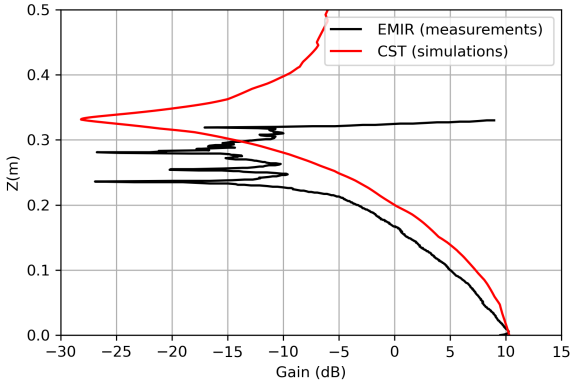

FIGURE 9. Simulated and measured gain at 1.1 GHz along a line lying in the vertical plane (Kapton film at X=59 cm from the monopole)

method consists in submitting a weakly conductive carbon-loaded Kapton film to the electric field, and then, induced currents in the film heat it by Joule effect. An infrared camera records this heating and provides field patterns. The microwave source is modulated at low frequency and through signal processing techniques including demodulation of the recorded images, to eliminate convection noise (lock-in technique). The infrared pictures obtained exhibit electric power profiles and, by square rooting, electric field frames. This is particularly suitable here to obtain the metamaterial SIS near field visualization.

The SIS efficiency was measured by moving the film and the camera together, in order to maintain the same focal length as shown on the EMIR setup in Fig. 10. The first position corresponds to the film placed at X = 9 cm from the monopole, the last position is at X = 1 m. The incident power supplied to the monopole is 5 W. The carbon loaded kapton film (Z_s = 1500 Ω) absorbs a fraction of the incident energy P_i which depends on its surface impedance Z_s. The absorption rate is given by:

$$A = 4.Z_s.Z_0/(Z_0 + 2.Z_s)^2 \tag{6}$$

where Z_0 =377 Ω is the free space wave impedance. As a result, 20 % of the incident power P_i is absorbed by the film and converted into heat. Finally, the power density absorbed by the film P_{abs} is proportional to the electrical field E following the relationship:

$$P_{abs} = \frac{E^2}{Z_s} \tag{7}$$

The EMIR measurement shows an amplification of 10 dB when the film is placed at X=59 cm from the monopole and of 7 dB at X=79 cm corresponding to a distance of one wavelength from the extremity of the metasurface (Figures 8, 9, and 11). The further the film is from the monopole, the lower the power absorbed by the film, demonstrating the limit of the range of use of the EMIR method for the electric field E_i measurement. This explains the 1 dB gain difference between the simulations and measurements observed in Fig. 8 for a distance greater than or equal to X=79 cm. Conversely, we observe a very good agreement between simulations and measurements when the film is closer to the monopole, particularly for film movement above the SIS. The measured gain is obtained by dividing the field measured with and without SIS. Through this ratio, measurement inaccuracies (related to the instruments) can offset each other or, on the contrary, amplify the deviation. This explains why, at certain points, the measured gain is slightly different from the simulated gain. However, we observed an average deviation of less than 10 % over the entire movement of the sensor.

IV. CONCLUSION

In this paper, the capability of increasing and confining the electric field radiated by a monopole antenna with a metamaterial super-inductive surface of limited thickness ($\lambda/30$) in the L-band has been demonstrated. A SIS mockup was designed and manufactured. Electromagnetic infrared measurements confirmed amplification levels of around 10 dB at the extremity of the metasurface and 7 dB at one wavelength further. This development is a valuable step forward for future developments in HF-band surface wave-launchers.

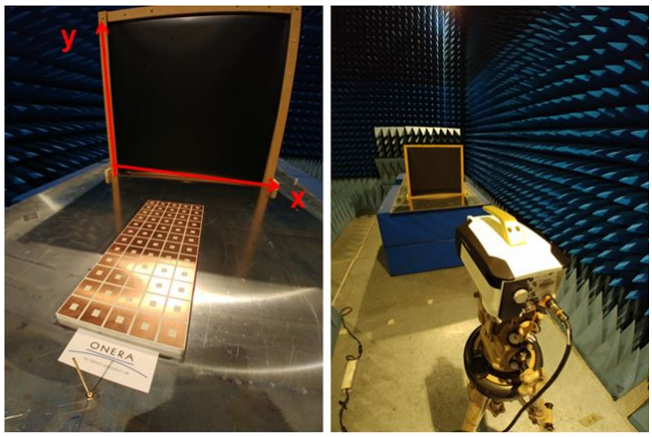

FIGURE 10. EMIR setup: ground plane, monopole, inductive metasurface, Kapton film, infrared camera

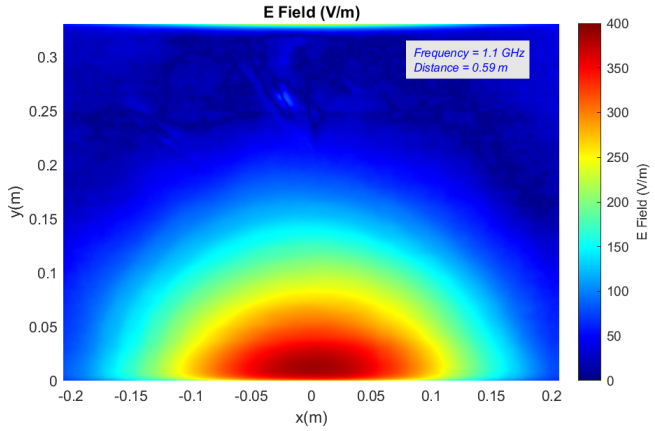

FIGURE 11. EMIR electric field measured at a distance of X=59 cm from the monopole

ACKNOWLEDGMENT

This work was supported by the French Ministry of Defense (DGA/AID) through the AC3M Rapid research project.

REFERENCES

[1] Ponsford, A.M and D-Souza, I.A and Kirubarajan, T., "Surveillance of the 200 nautical mile EEZ using HFSWR in association with a spaced-based AIS interceptor," Proc. IEE Conference on Technologies for Homeland Security (HST'09)., pp. 87-92, May 2009.

[2] Norton, K.A, "The Propagation of Radio Waves Over The Surface Of The Earth And In The Upper Atmosphere," Proceedings of the Institute of Radio Engineers., vol. 24, pp. 1203-1236, 1937.

[3] Roshn Entezar, S. and Namdar, A. and Rahimi, H., and Tajalli, H., "Localized Waves at the surface of a single-negative periodic multilayer structure," Journal of Electromagnetic Waves and Applications., vol. 23, no. 1, pp. 171-182, May 2019.

[4] Petrillo, L. and Jangal, F. and Darces, M. and Montmagnon, J-L and Hélier, M., "Negative Permittivity Media Able to Propagate a Surface Wave," Journal of Electromagnetic Waves and Applications., vol. 23, no. 1, pp. 171-182, May 2019.

[5] CST Microwave Studio, [Online]. Available: https://www.cst.com

[6] CIRETEC Elvia PCB, [Online]. Available: https://www.pcb-elvia.com/en/presentation/ciretec-2/

[7] Rogers TMM6 laminates, [Online]. Available: https://www.rogerscorp.com

[8] Ferreira, D. and Caldeirinha, R. and Cuinas, I. and Fernandes, R. "Square Loop and Slot Frequency Selective Surfaces Study for Equivalent Circuit Model Optimization., vol. 63, pp. 3947-3955, May 2015.

[9] Petrillo, L. and Jangal, F. and Darces, M. and Montmagnon, J-L and Hélier, M., "Towards a better excitation of the surface wave," Progress In Electromagnetics Research., vol. 13, pp. 17-28, May 2010.

[10] Jangal, F. and Bourey, N. and Darces, M. and Issac, F. and Hélier, M., "Observation of Zenneck-Like Waves over a Metasurface Designed for Launching HF Radar Surface Wave," International Journal of Antennas and Propagation., vol. 13, pp. 17-28, 2016.

[11] Jangal, F. and Petrillo, L. and Darces, M., "Inductive surface element," FR Patent FR20120002272 20120822., 2013.

[12] Levesque, P. and Leylekian, L., "Capteur de champ Electromagnetique par thermographie infrarouge," FR Patent 9816079, 1998., 1998.

[13] D.L. Balageas, D/L and Levesque, P. and DÃl'om, A., "Characterization of electromagnetic fields using lock-in IR thermography," Thermosense XV, SPIE., pp. 274-285, 1993.

[14] Prost, D. and Issac, F. and Martel, C. and Capet, N. and Sokoloff, J. and Pascal, O., "Electric field imaging of a high impedance surface for GNSS array decoupling application," European Physical Journal Applied Physics., vol. 72:11001, pp. 1-7, 2015.

[15] Crepin, T. and Issac, F. and Bolioli, S. and Prost, D., "Microwave electric field imaging of metamaterials using thermoemissive films," IEEE Antennas and Propagation Magazine., vol. 56, pp. 1-7, 2014.